

Analog Pink Noise Generator

Project Report

Team Members: Mason Bane, Cameron Osborne

ELEN 3445- Electronics 1

I. INTRODUCTION

The primary goal of this project is to design, simulate, build, and test a circuit that produces pink noise, that is, noise characterized by a power spectral density (PSD) decaying at -3 dB/octave centered at 0V DC, with a user adjustable output amplitude of 2V peak. Our final design uses a bipolar junction transistor (BJT) as the source of white noise, which is then shaped by a passive RC filter network to achieve the desired pink noise characteristics. This report aims to detail the technical background, design and simulation process in LTSpice, the challenges and design modifications performed along the way, and finally, the measured performance of our final circuit design.

II. TECHNICAL BACKGROUND AND DESIGN CONTEXT

A. What is Pink Noise?

Noise is characterized by chaotic or irregular vibrations and is often unwanted and undesired in communication [1]. However, it is in cases like these where we can use noise to our advantage. There are a few common types, called “colors” of noise, generated by capturing noise at different slopes ranging from -6dB to +6dB [1][2]. All of these colors of noise are generated from white noise, which has a slope of 0 dB/octave [1][2]. These colors of noise include Violet (+6 dB/octave), Blue (+3 dB/octave), Pink (-3 dB/octave), and Brown (-6 dB/octave). Pink Noise, also called 1/f or flicker noise, is characterized by a proportional decrease in power as the frequency increases, which is also referred to as having ‘equal power per octave’ [1][2]. It is due to these characteristics that pink noise can be described as sounding flatter and less harsh than white noise [1].

B. Common Pink Noise Applications

Pink noise occurs naturally in the forms of oceans waves and wind, which are seen as soothing; it is for this reason pink noise is used as both a therapy tool and a sleep aid [1][3]. Along with its pleasant sound, pink noise

is a valuable tool for various audio engineering tasks due to its ability to mimic the human auditory system [1][2], most commonly used for speaker calibration and equipment testing to detect unwanted frequency response across the entire spectrum of human hearing (20Hz - 20 kHz) [1][4].

C. General Theory of Pink Noise Generation

The working theory for generating pink noise involves a three-stage process. First white noise is generated, typically via a reverse-biased bipolar junction transistor (BJT) [5]. The white noise is then passed through a resistor-capacitor network to attenuate the signal's power spectral density (PSD) slope to -3 dB/octave, effectively changing the noise from “white” to “pink” [1][5]. Finally, the resulting pink noise voltage can be significantly weaker due to noise suppression. In order to counteract this effect, a gain stage is applied to amplify the final voltage to a more audible, usable level [5].

D. Comparison of Analog and Digital Pink Noise Generator Circuits

Along with analog pink noise generation using the three-stage process mentioned in the previous section, there is also another similar process for pink noise generation via digital signals. Digital pink noise generation follows a two-stage process. This process starts with white noise generation via an evenly distributed pseudo-random number generator (PRNG) which produces a series of values representing the power across all frequencies, forming a discrete white noise signal. The white noise is then digitally filtered by applying filtering algorithms to these values to reduce the power slope from evenly distributed to the 1/f frequency that characterizes pink noise [1][5]. In both systems, there are most definitely a few tradeoffs. While digital pink noise is much simpler to produce, it lacks the true randomization that would be present in an analog model. That said, an analog model is also not perfect due to its susceptibility to unwanted effects generated by individual component tolerances and other factors, preventing the analog pink noise from being as stable or precise as its digital counterpart.

E. LTSpice Limitations and Work Arounds

The main issue found in circuit simulation is that LTSpice is not able to model the white noise generation stage using the BJT due to the lack of breakdown voltages in the model used in LTSpice [7][8]. This directly affects our transient (time-domain) testbench since we cannot generate a noise source in the same way that our actual implementation would. Even if this was possible, the AC testbench could not work due to the fact that noise generation occurs in the time domain, not a frequency domain, so when an AC simulation (a frequency domain simulation) is run in LTSpice, it cannot process the noise waveform at all.[7]-[9]. The workaround that we chose for this is that it is possible to generate and use a white noise .wav file as an input via a voltage source [10]. Also present in LTSpice are three parameter functions that can be used to generate noise, RAND(), RANDOM(), and WHITE(), which all produce digitally generated white noise similar to the method described in the previous section [10]. Each of these produces noise at a peak-to-peak voltage of 1V with different characteristics, the RAND() function generates voltages that tend to be more square and not smooth [10]. The RANDOM() function produces a smoothed noise but has a DC offset by default [10]. Finally, the WHITE() function produces a similarly smoothed noise, without the DC offset, which could be suitable for use in the simulation [10]. For AC simulations, it is possible to use the noise on a voltage source to set the output voltage source, the input source, the type of sweep, the number of points per decade/octave, and the start and stop frequency [11]. This will produce a usable noise in our circuit for analysis at the input source [11].

F. Transistors and Diodes as Functional Noise Sources

While researching alternatives to white noise generators, we found that others have used BJT transistors with a reverse biased source on the base pin with an open emitter pin, and the collector pin is followed by a resistor to the forward biased source [12]. BJT's have been found to vary a great amount even though they models are the same or from the same production line. This is because as the device geometries are scaled down the low-frequency noise will strongly deviate from a $1/f$ behaviour due to the presence of g-r centers,

therefore the noise generated between each BJT is unpredictable and varies greatly.[12] Others have also used what is called a “Reverse-Biased Zener Diode” [13]. Which is a specialized diode that is connected in reverse bias direction once a specific voltage, known as the Zener or “breakdown” voltage, is reached; it creates white noise [13]. The Zener diode behaves like a normal diode when it is in the forward bias. When both sides of a diode are heavily doped, the depletion region becomes very narrow and under reverse bias, a strong electric field develops across this narrow region [13]. As the reverse voltage increases and the field becomes intense enough, it breaks covalent bonds and frees many charge carriers [13]. Near the Zener voltage, the electric field is strong enough to pull electrons from their valence bands, causing a sudden, sharp increase in current with only a small rise in voltage [13].

III. DESIGN METHODS

We initially wanted to do many RC shelves in our design but soon found that the implementation of this would be costly in money and time. This would also add to the complexity of the attenuation of higher pitch noise to create the desired decibel(dB) per octave roll-off of -10dB per decade or -3dB per octave. Using the standard frequency shelf method gave us three significant advantages. First of which it has a simple implementation and therefore simple troubleshooting. Secondly, it gives us a more predictable gain behaviour as it is easier to dial in consistent tonal changes and is less sensitive to order/pole count than other designs. Thirdly, it allows us to have frequency limited attenuation without complete cutoff while preserving the timbre and controlling the higher brighter notes.

A. Overview of Design Architecture and Approach

A pink noise filter is built by first generating broadband white noise using a reverse biased BJT transistor source and then shaping its waveform, so it follows the characteristic -3 dB per octave ($1/\sqrt{f}$) attenuation curve. After filtering, the signal is typically normalized to ensure consistent output levels and to prevent clipping, and stability handling may be added depending on the use case. The design process involves defining performance

requirements, given that we are creating a pink noise filter that has no purpose other than to be listened to, we decided simplicity is king when it comes to cost v.s. time of implementation and troubleshooting.

B. Justification of Discrete Battery Type and Chosen Voltage Levels

We decided to use dual 9V batteries in series as these are common and reliable and give us the minimum voltage, we selected our parts for. This gives us a voltage differential total of 18V well above the minimum for our TL072CP Operational Amplifier and above the 9V threshold for our BC337-16 BJT transistor. The resistors were chosen to have a difference of $\pm 1\%$, so we have fewer unknown variables when it came to troubleshooting our circuit. The capacitors were chosen for their robust voltage capacity as well as their accuracy although the lowest tolerances of some of the capacitors were in the $\pm 20\%$ range.

C. Design Challenges and Methods

I found the white noise generation stage to be the most difficult part of the project due to the variance or in this case the invariance of the BJT transistors used to create the white noise. These BJT transistors were quiet across all of the ones I ordered causing the noise to be significantly lower than it should be. If we try to gain up a low amount of white noise, we will not have much at the output even with an $11V/V$ gain factor. This in turn caused the final output to the piezoelectric speaker to be magnitudes less than it should be. We were able to gain up the little noise we had by increasing the gain by 2 whole magnitudes. We were able to do this by replacing the feedback resistor of $100k\Omega$ in the gain stage with a $10Meg\Omega$. This got the speaker up to the $2V$ minimum for the max voltage output when the potentiometer was tuned all the way up. However, this caused the nicer softer pinker noise we were getting pre-replacement, to be harsher and whiter.

IV. SIMULATED RESULTS

Displayed in figure 1 is design for the entire circuit from white noise generation using the BJT transistor to gain it up with the first TL072CP OpAmp and then filtering out the unwanted frequencies in the second

TL072CP OpAmp. In the LTspice simulations, our design achieved an output of 1V peak or 2V peak to peak, shown in figure 2 from our transient testbench, which is still within the design parameters of the project. Figure 3 shows that the values of the frequencies are centered on 0.00 volts and therefore are not shifted up or down causing abnormalities at the output.

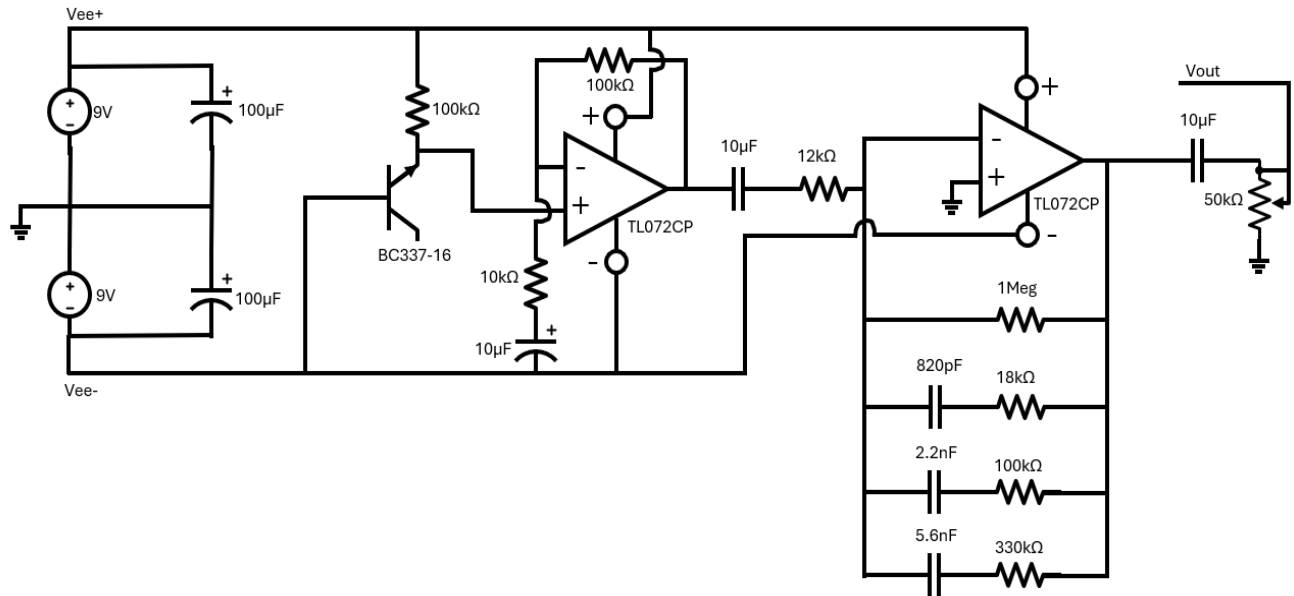


Figure 1

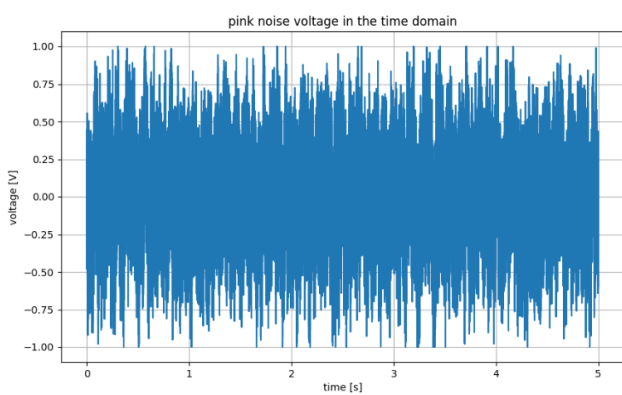
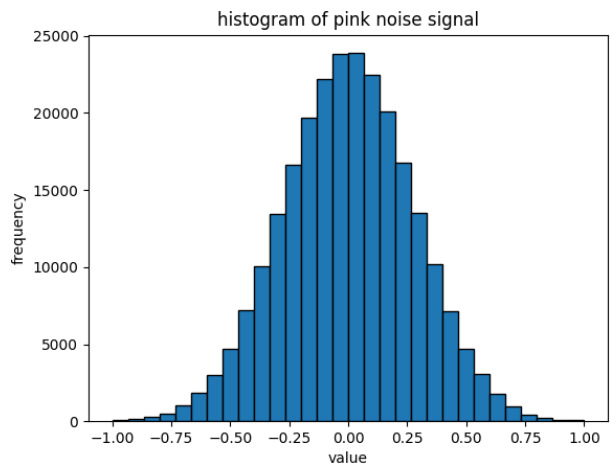


Figure 2.) (Left)
Figure 3.) (Right)



Below is the power spectral density from our design shown in figure 4 and figure 5. Both are close to ideal in slope but not perfect due to the limited number of shelves in our design.

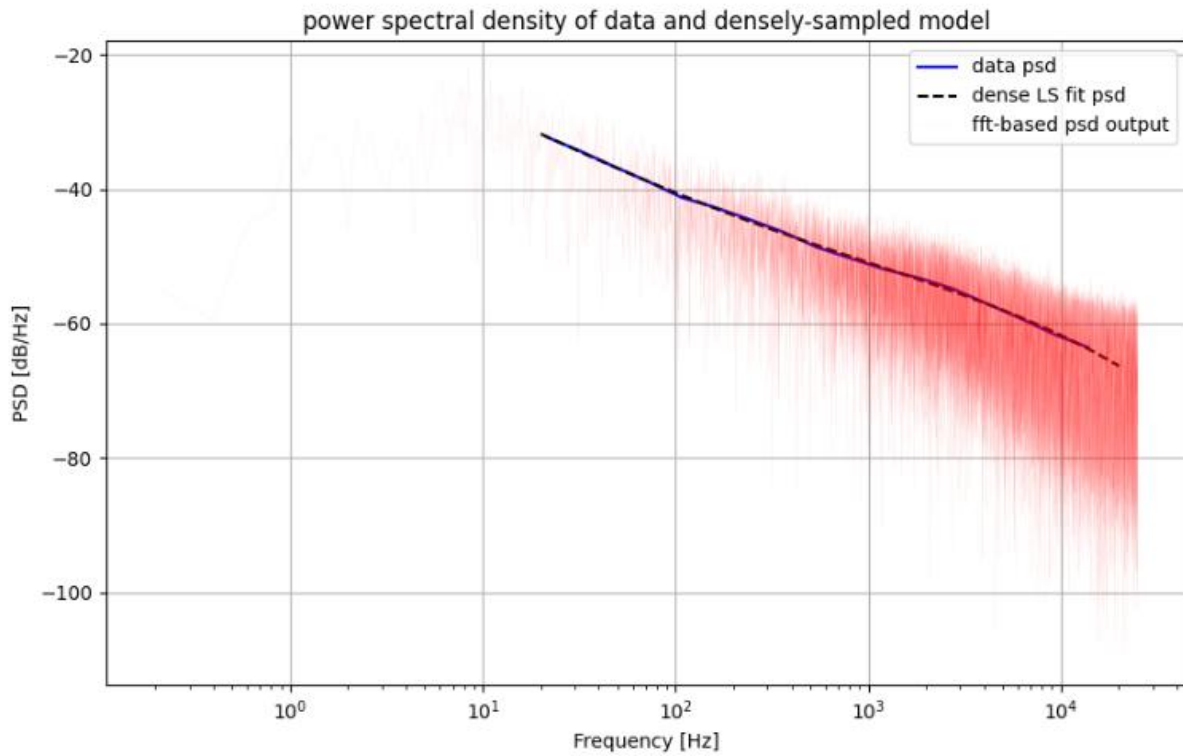


Figure 4

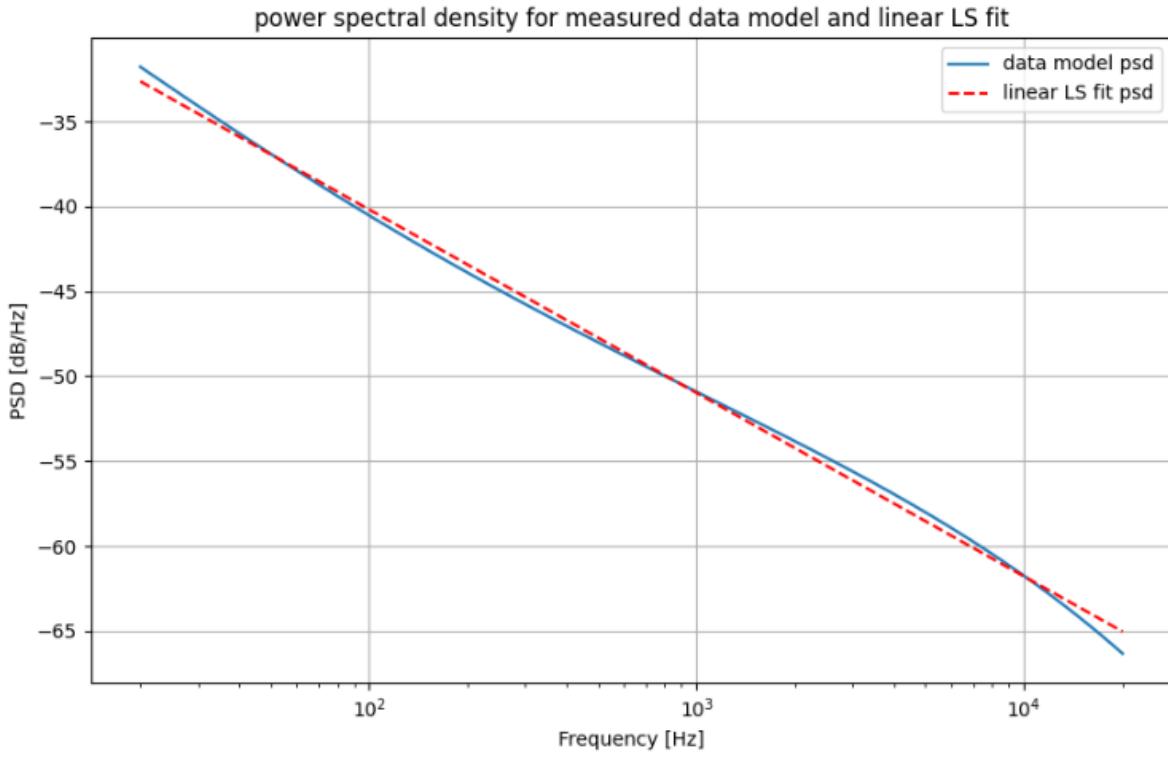


Figure 5

From the shaping filter testbench in Ltspice you can clearly see the roll off from the starting value of 35db in the solid red line and the phase in the dotted red line in figure 6. Figure 7 shows the output from python code output using our Vout data from Ltspice as the input. Both are similar in slope and shape with a roughly -3dB per octave roll off.

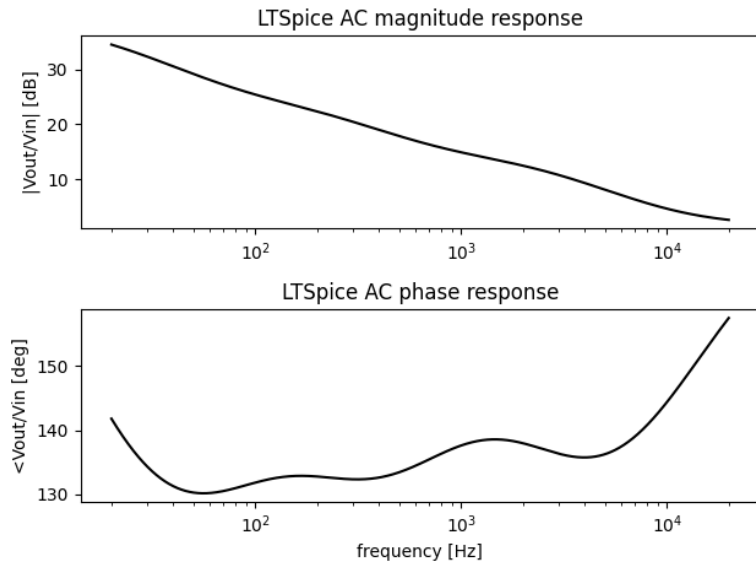


Figure 6

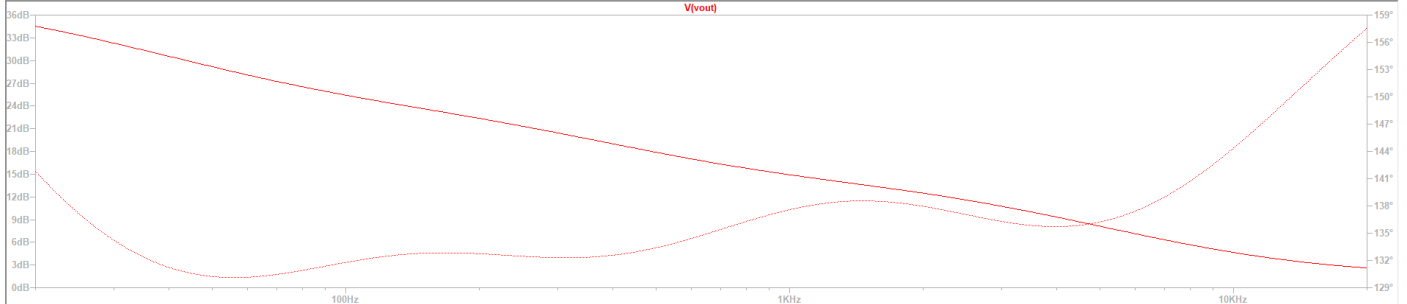


Figure 7

From the AC testbench in figure 8, you can see the Power Spectral Density (PSD) response. It aligns very well with the previous slopes from the other testbenches and python outputs.

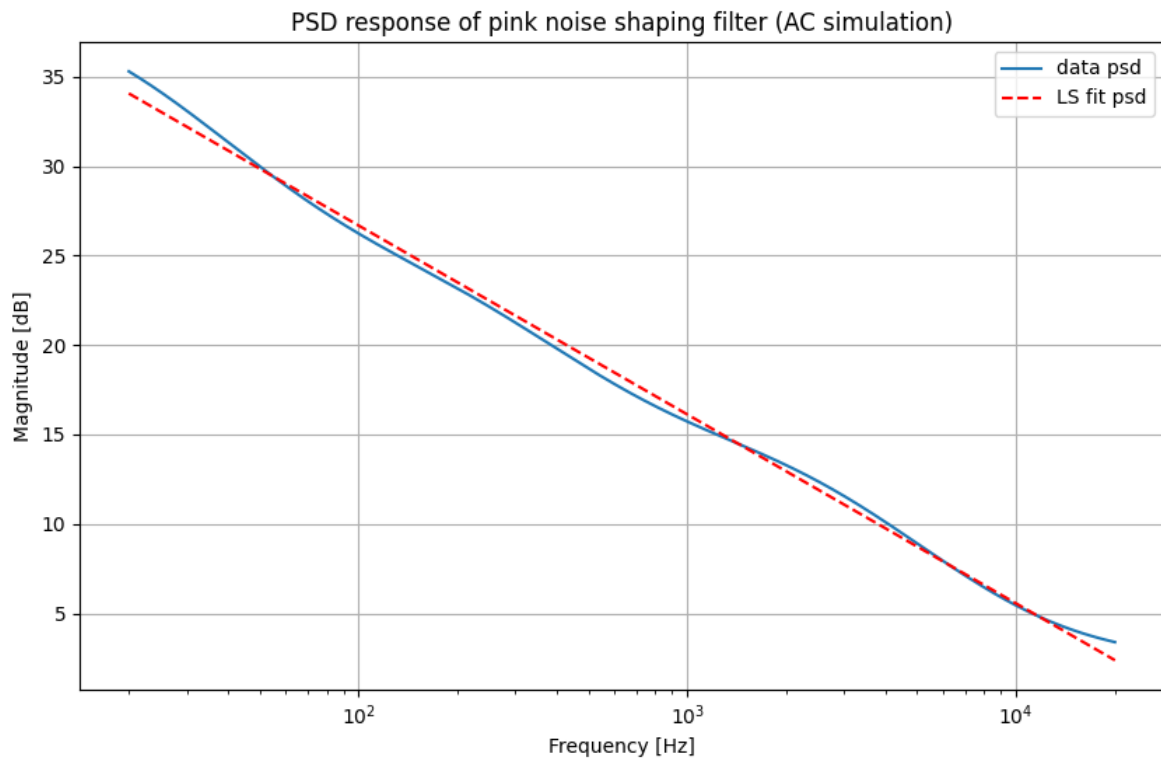


Figure 8

A. Initial Simulated Performance Using a White Noise Voltage Source

We found that the simulated results were on par with the project's end goal. It provided a -3dB/octave slope and closely followed the ideal line shown in the figures 4, 5, 8, previously mentioned above.

B. Final Design Changes Implemented

We had trouble getting the proper amount of voltage at the output for the piezoelectric speaker so I changed the feedback resistor to be 2 magnitudes above the original value of $100\text{k}\Omega$, $10\text{Meg}\Omega$. This essentially forced the output to be within the specified range but at the cost of quality of the pink noise output.

C. Final Circuit Schematic and List of Components

Seen in figure 9, our final design schematic did not change hardly anything from the initial design except the value of the $100\text{k}\Omega$ feedback resistor to a $10\text{Meg}\Omega$ resistor.

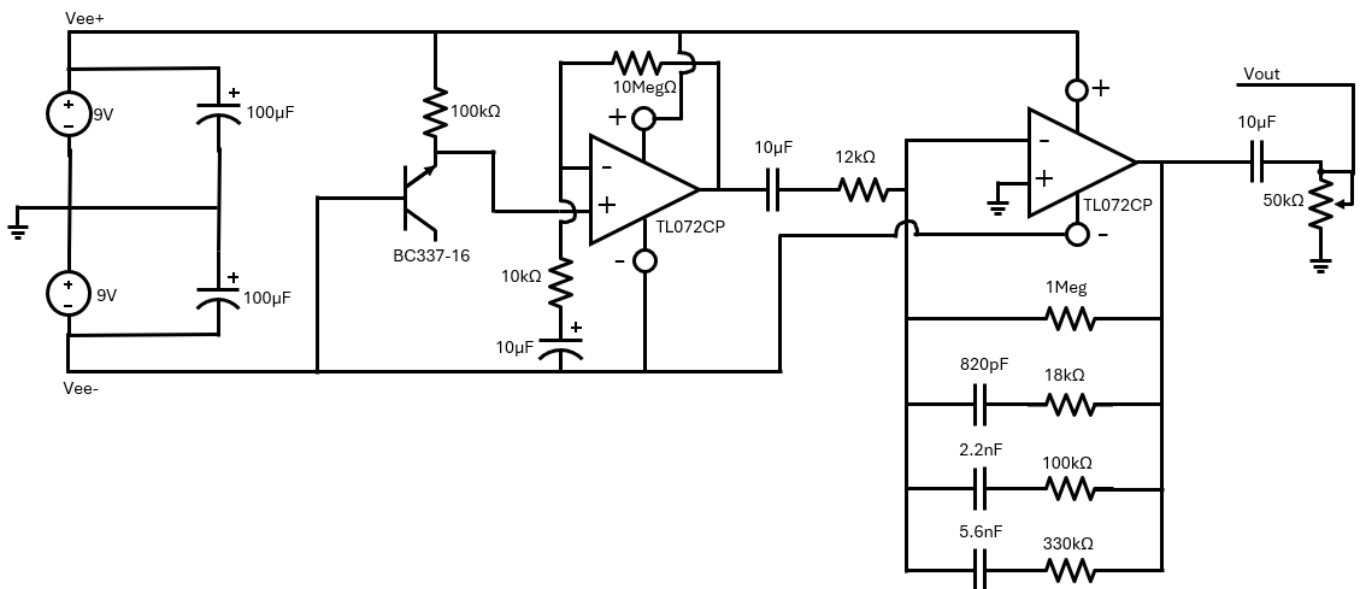


Figure 9

Below is a list of all of our components and their cost:

- TL072CP \$0.35x2 = \$0.70
- BC337-16 \$0.17x1 = \$0.17
- 9V Battery \$7.99x2 = \$14.98
- 10μF Electrolytic Capacitor \$0.65x1 = \$0.65
- 100μF Electrolytic Capacitor \$0.50x2 = \$1.00

• 10 μ F Non-Polarized Capacitor	\$1.76x1 = \$3.52
• 820pF Non-Polarized Capacitor	\$0.35x1 = \$0.35
• 2.2nF Non-Polarized Capacitor	\$0.21x1 = \$0.21
• 5.6nF Non-Polarized Capacitor	\$0.37x1 = \$0.37
• Resistors $\pm 1\%$ (Combined Cost of All)	\$0.10x8 = \$0.80
• Potentiometer Type A	\$2.00x1 = \$2.00
• Piezoelectric Speaker	\$9.69x1 = \$9.69
• Wire(approx. per foot)	\$0.10x2 = \$0.20
• Breadboard	\$7.99x1 = \$7.99

This brought our total to 42.63 or 46.04 with a 8% tax rate included. This cost can be brought down as components are usually bought in bulk so these rates should be considered at the high end of cost per product since they are mass produced. In addition to this, a significant amount of the cost burden could be handled by the replacement of the breadboard with a custom designed circuit board and a power supply.

D. Measured Performance Report for Final Schematic

The final measurement results for our circuit are listed below from the outputs of our python script:

p value for lp-norm: **2**

measured data psd slope error: **171.71280565598002e-3**

measured data lp-norm psd error: **142.61849780349598**

measured project score (the lower, the better): **145.16**

Below are the real world outputs of the circuit we created shown in figures 10-14

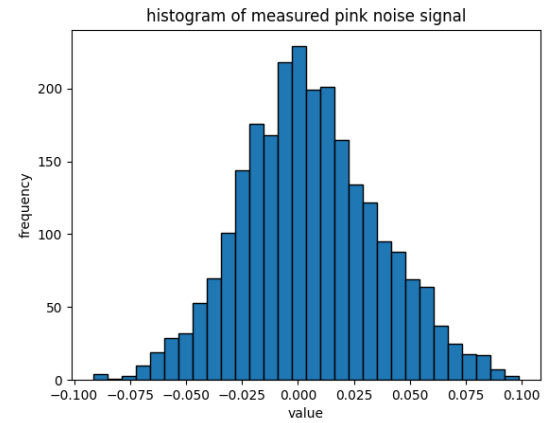
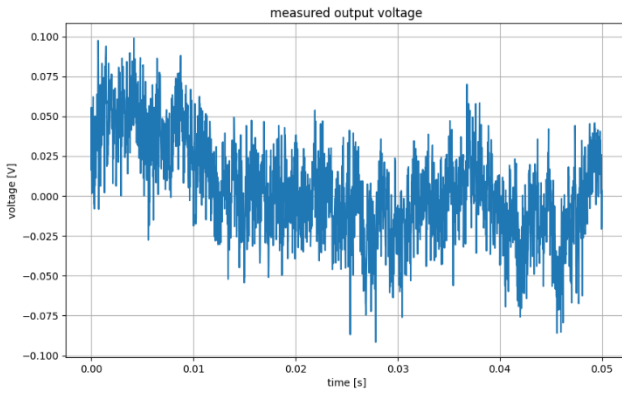


*Figure 10.) (Left)
Figure 11.) (Right)*

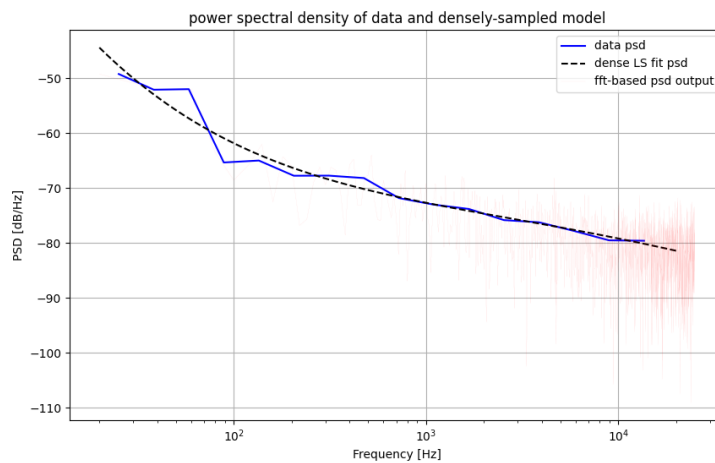
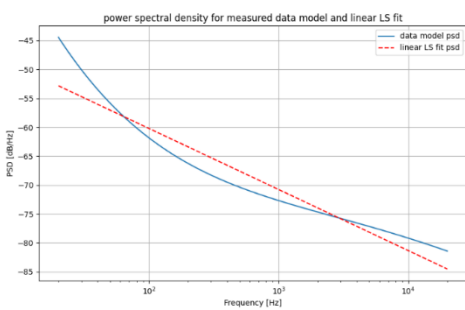
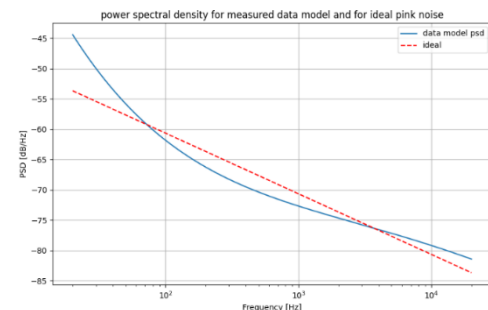


Figure 12.) (Left)



*Figure 13.) (Left)
Figure 14.) (Right)*



V. CONCLUSION

Overall, the design and implementation of our pink noise filter demonstrated the importance of balancing theoretical ideals with practical engineering constraints. Although an initial multi-shelf RC approach was considered, the complexity, cost, and difficulty of achieving an accurate -3 dB per octave slope led us to adopt a simplified shelf-based architecture that offered predictable gain behavior, easier troubleshooting, and a more efficient build. Using a reverse-biased BJT transistor to generate white noise and shaping it with a TL072CP-based filter allowed us to meet the core design objective, though challenges arose from the unexpectedly low noise output of the transistors, which required a significant increase in amplification. This modification successfully brought the output to the required voltage level, but at the expense of some spectral softness, pushing the noise closer to white than ideal pink. Simulated and measured results confirmed that the circuit achieved a close approximation of the target roll-off, with performance scores and PSD slopes aligning reasonably well with expectations given the limited number of shelves and the simplified architecture. Despite minor changes necessary to reach a functional output, the final design met the fundamental project requirements, remained cost-effective, and provided a clear understanding of the tradeoffs involved in analog pink noise generation.

REFERENCES

- [1] G. Eason, B. Noble, and I. N. Sneddon, “On certain integrals of Lipschitz-Hankel type involving products of Bessel functions,” *Phil. Trans. Roy. Soc. London*, vol. A247, pp. 529–551, April 1955. (*references*)
- [2] J. Clerk Maxwell, *A Treatise on Electricity and Magnetism*, 3rd ed., vol. 2. Oxford: Clarendon, 1892, pp.68–73.
- [3] I. S. Jacobs and C. P. Bean, “Fine particles, thin films and exchange anisotropy,” in *Magnetism*, vol. III, G. T. Rado and H. Suhl, Eds. New York: Academic, 1963, pp. 271–350.
- [4] K. Elissa, “Title of paper if known,” unpublished.
- [5] R. Nicole, “Title of paper with only first word capitalized,” *J. Name Stand. Abbrev.*, in press.
- [6] Y. Yorozu, M. Hirano, K. Oka, and Y. Tagawa, “Electron spectroscopy studies on magneto-optical media and plastic substrate interface,” *IEEE Transl. J. Magn. Japan*, vol. 2, pp. 740–741, August 1987 [Digests 9th Annual Conf. Magnetics Japan, p. 301, 1982].
- [7] M. Young, *The Technical Writer’s Handbook*. Mill Valley, CA: University Science, 1989.
- [8] K. Eves and J. Valasek, “Adaptive control for singularly perturbed systems examples,” Code Ocean, Aug. 2023. [Online]. Available: <https://codeocean.com/capsule/4989235/tree>
- [9] D. P. Kingma and M. Welling, “Auto-encoding variational Bayes,” 2013, arXiv:1312.6114. [Online]. Available: <https://arxiv.org/abs/1312.6114>
- [10] S. Liu, “Wi-Fi Energy Detection Testbed (12MTC),” 2023, GitHub repository. [Online]. Available: <https://github.com/liustone99/Wi-Fi-Energy-Detection-Testbed-12MTC>
- [11] “Treatment episode data set: discharges (TEDS-D): concatenated, 2006 to 2009.” U.S. Department of Health and Human Services, Substance Abuse and Mental Health Services Administration, Office of Applied Studies, August, 2013, DOI:10.3886/ICPSR30122
- [12] M. Sandén, “A new model for the low-frequency noise and the noise level variation in polysilicon emitter BJTs,” *IEEE Transactions on Electron Devices*, vol. 49, no. 3, pp. 514–520, Mar. 2002, doi: 10.1109/16.987124.
- [13] S. Mane, “Zener Diode: Theory, Applications, and Advancements,” vol. 11, no. 9, pp. 1392–1397, Sept. 2023.